

Formation mechanism of steep convergent intracontinental margins: Insights from numerical modeling

Lin Chen,^{1,2} Taras V. Gerya,² Zhong-Jie Zhang,¹ Alan Aitken,³ Zhong-Hai Li,⁴ and Xiao-Feng Liang¹

Received 22 February 2013; revised 3 April 2013; accepted 3 April 2013; published 30 May 2013.

[1] The margins surrounding the Tibetan Plateau show some diversity in topographic gradient. The most striking example is the eastern Tibetan margin bordered by the Longmen Shan range, which is characterized by a remarkably steep topography transition between eastern Tibet and the Sichuan Basin. There is significant uncertainty over whether this margin was formed by crustal shortening or lower-crustal flow. To investigate the formation mechanism of steep convergent intracontinental margins, we conducted petrological-thermomechanical numerical simulations based on the lithospheric structure and thermal state of the eastern Tibetan margin. Our numerical experiments demonstrate that a very steep topographic gradient, such as the eastern Tibetan margin, is an inherent characteristic of convergence between a hot and weak lithosphere with thick crust and a cold and strong lithosphere with thin crust. Although lower-crustal flow has potentially contributed to the crustal thickness difference between the two convergent blocks, it is not a prerequisite for the growth of steep convergent intracontinental margin. Rather, the topography at the margin can be explained by a near isostatic response to crustal thickening resulting from shortening. **Citation:** Chen, L., T. V. Gerya, Z.-J. Zhang, A. Aitken, Z.-H. Li, and Liang X.-F. (2013), Formation mechanism of steep convergent intracontinental margins: Insights from numerical modeling, *Geophys. Res. Lett.*, 40, 2000–2005, doi:10.1002/grl.50446.

1. Introduction

[2] The Cenozoic collision between Indian and Eurasian continents has created the largest and highest plateau on earth, the Tibetan Plateau [e.g., *Yin and Harrison, 2000*]. Despite its great elevation, the interior of the plateau is remarkably flat [e.g., *Fielding et al., 1994*]. In comparison with the flat hinterland, the northern and eastern Tibetan margins bounded by cratonic blocks, such as the Sichuan and Tarim Basins, are characterized by sharp topography

transitions. For example, topography goes from ~500 m in the Sichuan Basin to more than 5000 m in the plateau over a horizontal distance of less than 50 km (Figure 1c), where the Longmen Shan range (LMS) marks the border between the Sichuan Basin and eastern Tibet. GPS measurements demonstrate that the recent surface convergence rate in the LMS region is strikingly low (less than 3 mm/a, e.g., *Gan et al. [2007]*). Geological observations also suggest that large-scale crustal shortening is not significant in late Cenozoic history of this area, with only 10–20 km reported [*Burchfiel et al., 1995, 2008*]. Due to this apparent lack of shortening, topographic growth in east Tibet has commonly been explained by the inflation of the ductile lower crust beneath the plateau edge by gravitational potential energy-driven eastward flow of the lower crust from the central plateau [*Royden et al., 1997; Meng et al., 2006*].

[3] Several recent studies in eastern Tibet have challenged the dominance of the lower-crustal flow hypothesis on the basis of some new observations. *Wallis et al. [2003]* demonstrated the existence of a previously unknown region of circa 65 Ma Barrovian-type metamorphism in central Longmen Shan, with peak metamorphic conditions of ~8 kbar and ~700°C. This was interpreted to suggest that the crust beneath the LMS was already thick at the time of the India-Asia collision. *Hubbard and Shaw [2009]* used balanced geologic cross-sections to show that post-Jurassic crustal shortening and topography are strongly correlated in the LMS front, thus suggesting that crustal shortening was the primary driver for the uplift of the LMS, although their analysis lacked direct constraint on when this shortening occurred. Thermochronology in this region [*Wang et al., 2012*] suggests a two-phase growth of the Longmen Shan, with slow, steady exhumation in the early Cenozoic and two rapid pulses of exhumation beginning at 30–25 Ma and ~10 Ma. Crucially, this work supports significant topographic growth prior to the Indo-Asian collision, and the 30–25 Ma acceleration of exhumation is considered too close to the time of collision to be plausibly explained by lower-crustal flow.

[4] Seismic studies reveal distinct differences in the lithosphere across the eastern Tibetan margin, including a decrease in crustal thickness from ~60 km beneath eastern Tibet to ~40 km beneath the Sichuan Basin [*Wang et al., 2007; Zhang et al., 2009; Robert et al., 2010*]. Seismic tomography results suggest that lithosphere beneath eastern Tibet is hot, and the Sichuan Basin is cold [*Li et al., 2006*]. Receiver function results also show that the lithosphere-asthenosphere boundary (LAB) beneath eastern Tibet is significantly shallower than that beneath the Sichuan Basin [e.g., *Zhang et al., 2010; Hu et al., 2011*].

¹State Key Laboratory of Lithospheric Evolution, Institute of Geology and Geophysics, Chinese Academy of Sciences, Beijing, China.

²Institute of Geophysics, Swiss Federal Institute of Technology (ETH-Zurich), Zurich, Switzerland.

³Centre for Exploration Targeting, The University of Western Australia, Crawley, WA, Australia.

⁴State Key Laboratory of Continental Tectonics and Dynamics, Institute of Geology, Chinese Academy of Geological Sciences, Beijing, China.

Corresponding author: L. Chen, State Key Laboratory of Lithospheric Evolution, Institute of Geology and Geophysics, Chinese Academy of Sciences, Beitucheng West Road No. 19, Chaoyang District, Beijing 100029, China. (chenlin@mail.iggcas.ac.cn)

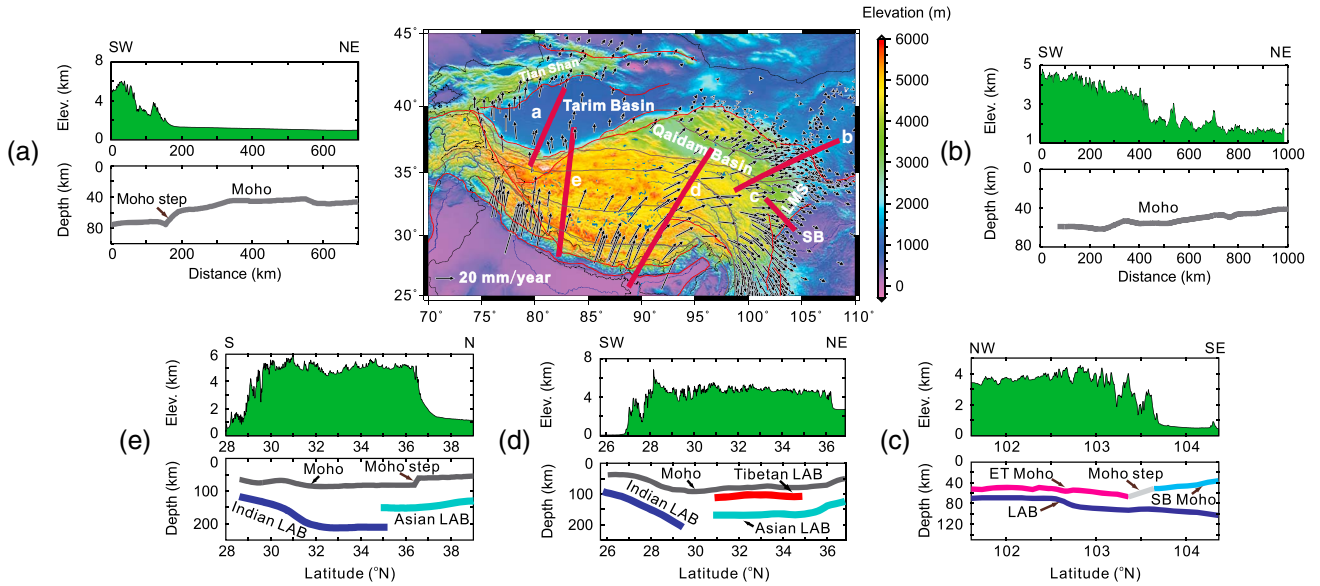


Figure 1. Topography map of the Tibetan Plateau. (a, b, c, d, and e) Thick solid lines indicate profiles with topography and crustal/lithospheric structure across the margins of the plateau. Dark arrows denote observed GPS velocity vector [Gan *et al.*, 2007]. Figure 1a is derived from Xiao *et al.* [2002]; Figure 1b is derived from Liu *et al.* [2006]; Figure 1c is derived from Zhang *et al.* [2009, 2010]; Figure 1d is derived from Zhao *et al.* [2011]; and Figure 1e is derived from Zhao *et al.* [2010]. SB stands for the Sichuan Basin.

[5] These significant contrasts in the lithospheric structure and thermal state between the plateau and adjoining basins cause substantial differences in buoyancy forces; thus, they are likely to play important roles in the formation of a steep topographic margin. In order to explore the impact of these differences on processes at intraplate margin with steep topography, we conducted petrological-thermomechanical numerical simulations to examine the influences of lateral variations in the structure and thermal state of the lithosphere on mountain building. The main idea is to investigate the dominating factors controlling the formation of steep intracontinental margins. For clarification purpose, we emphasize that a steep intracontinental margin here indicates a sharp topography transition with high topographic gradient between plateau and cratonic basin in an intraplate setting. Although we use the eastern Tibetan margin as an example on which to base our numerical modeling, the north-Tibetan margin shows similar characteristics (Figure 1), and the model is broadly applicable to this margin also.

2. Numerical Model

[6] The numerical experiments were performed with the I2VIS code [Gerya and Yuen, 2003]. The code combines a

conservative finite difference method on a staggered grid with a nondiffusive marker-in-cell technique. A thermodynamic database is implemented, and different lithologies are endowed with plausible physical properties. The computational domain is 4000×1500 km. The non-uniform 1361×351 rectangular grid is designed with a resolution of 1×1 km for the interacting zone of two continental lithospheres and 10×10 km for the zones beside it. The mechanical boundary conditions of the model are free slip at all boundaries, except at the lower boundary (1500 km deep), which is treated as a permeable boundary satisfying an external free slip boundary condition [Burg and Gerya, 2005]. The initial temperature profile is assumed to linearly increase from 0°C at the surface to 1350°C at the base of the lithosphere. For example, for the lithosphere with a thickness of L , the initial temperature profile is given by $T(z) = z/L * 1350^\circ\text{C}$. When there is a transition zone between two convergent lithospheres with different thicknesses, the initial temperature at this region is calculated by linearly interpolating the isotherms of the neighboring regions. The initial temperature gradient in the asthenospheric mantle is $0.46^\circ\text{C}/\text{km}$. The upper thermal boundary is set to a constant temperature, and the lower thermal boundary is set to an external constant temperature condition that simulates an

Table 1. Material Property Used in Modeling^a

Rock type	Density (kg/m^3)	Thermal Conductivity ($\text{W}/\text{m}/\text{K}$)	Flow Law ^b	Cohesion (MPa)	Friction Angle ($\sin\phi$)
Sediment	2600	$0.64 + 807/(T + 77)$	Wet quartzite	1.0	0.15
Upper crust	2700	$0.64 + 807/(T + 77)$	Wet quartzite	1.0	0.15
Lower crust	2800	$0.64 + 807/(T + 77)$	Plagioclase An ₇₅	1.0	0.15
Lithospheric mantle	3300	$0.73 + 1293/(T + 77)$	Dry olivine	1.0	0.6
Asthenosphere	3200	$0.73 + 1293/(T + 77)$	Dry olivine	1.0	0.6
Weak zone	3200	$0.73 + 1293/(T + 77)$	Wet olivine	1.0	0.0

^a T denotes temperature.

^bFlow laws are taken from Ranalli [1995].

Table 2. Parameters and Results of Conducted Experiments^a

Model Name	ΔH_{crust} (km)	ΔH_{lith} (km)	ΔH_{sed} (km)	Comments
TOP1 (Model A)	15	20	Non	Steep margin
TOP2	15	Non	Non	Steep margin
TOP3 (Model B)	Non	20	Non	Underthrust
TOP4 (Model C)	Non	Non	Non	Underthrust
TOP5	15	20	3 km	Steep margin
TOP6	15	Non	3 km	Steep margin
TOP7	Non	20	3 km	Underthrust
TOP8	Non	Non	3 km	Underthrust

^a ΔH_{crust} , ΔH_{lith} , and ΔH_{sed} are thickness difference of crust, lithosphere, and sediment between the left and right boxes, respectively, where $\Delta H_{\text{crust}} = H_{\text{left}} - H_{\text{right}}$, $\Delta H_{\text{lith}} = H_{\text{right}} - H_{\text{left}}$, and $H_{\text{sed}} = H_{\text{right}} - H_{\text{left}}$. Models A and B are shown in Figures 2 and 3, respectively, and Model C is shown in Figure 4.

additional mantle volume present below the bottom of the model. Both lateral thermal conditions are insulating. The top surface of the crust is calculated dynamically as an internal quasi-free surface by employing a sticky air layer of low viscosity (10^{19} Pa s) and low density (1.0 kg/m^3). The interface between this weak layer and the top of the crust is treated as an internal erosion-sedimentation surface that evolves according to the transport equation solved at each time step.

[7] Our two-dimensional numerical models simulate the rheology of the lithosphere-upper asthenosphere section (Table 1) of the Tibetan Plateau margins as shown in Figure 1. Lithospheric and crustal structures used in models are referred to seismic imaging results reported by Zhang *et al.* [2009, 2010], Robert *et al.* [2010], Liu *et al.* [2006], and Xiao *et al.* [2002]. The initial temperature structure of the models is based on estimations of $\sim 1300^\circ\text{C}$ at depths of 80–100 km in the eastern Tibetan Plateau, reported by Holbig and Grove [2008]. Because we are focusing on the formation of steep-gradient topography during intraplate convergence rather than the entire convergence process, the crust in some setups is already prethickened, which is in agreement with the results of geological studies [Wallis *et al.*, 2003; Wang *et al.*, 2012]. The left part of the model represents the plateau, and the right side represents the cratonic basin (e.g., Sichuan Basin or Tarim Basin).

[8] Although erosion and sedimentation are important processes in the mountain building process [Avouac and Burov, 1996], to better concentrate on investigating the influence of preexisting contrasts in lithospheric structure and temperature between two converging intraplate blocks on mountain building, we set erosion/sedimentation rate in all models to be zero. Considering our modeling involves the convergence between plateau and cratonic basin, the preexisting contrast in sediment thickness between the two blocks is taken into account and is tested as an additional influence factor (e.g., Table 2). The whole system is driven by a constant convergence rate of 2.5 cm/a applied to the leftmost side of the model (Figure 2).

3. Results

[9] Eight numerical models, with variable thicknesses of the lower crust, lithospheric mantle, and sediment layers for the plateau side, were performed to systematically investigate the influence of lithospheric contrasts on the formation

of steep topography during intracontinental convergence (Table 2). Because initial temperature structure is controlled by the LAB depth, the lithospheric thickness also defines the difference of the thermal state.

[10] The models can be classified into two main modes as shown in Figure 3, which shows the composition field of Mode-I (e.g., TOP1, 2, 5, and 6 in Table 2) and Mode-II (e.g., TOP3, 4, 7, and 8 in Table 2) after 10 Ma of convergence. Figure 3a corresponds to the case of intensive convergence, without the development of plate subduction. In this case, a hot lithosphere with thick crust converges with a cold lithosphere with thin crust. The result of this is that the prethickened crust of the plateau overthrusts the thin crust of the cratonic basin. In this mode, lithospheric shortening is concentrated on the plateau side and is accommodated by upper crust overthrusting, lower crust buckling, and lithospheric mantle thickening. The cratonic basin block displays little deformation except for slight bending due to lithospheric flexure, in agreement with gravity modeling results [Fielding and McKenzie, 2012]. The crustal architecture is remarkably similar to the crustal structure for the eastern Tibetan margin [e.g., Zhang *et al.*, 2009; Robert *et al.*, 2010; also see Figure 1c] and also is consistent with the deep seismic sounding results across the western Kunlun fault in the northern Tibetan margin (e.g., Xiao *et al.* [2002]; also see Figure 1a). The present-day LAB depth of eastern Tibet reported by different authors show some diversity. The lithospheric architecture after 10 Myr's modeling is compatible with the results reported by Hu *et al.* [2011] (Figure 3a). Ongoing convergence leads to the building of steep topography at the margin of the two blocks (Figure 3a), with topographic profiles that resemble closely the observed profiles for the northern and eastern Tibetan margins (Figures 1a–1c).

[11] The alternative Mode II, with the same thermal contrast but without an initial crustal thickness contrast between

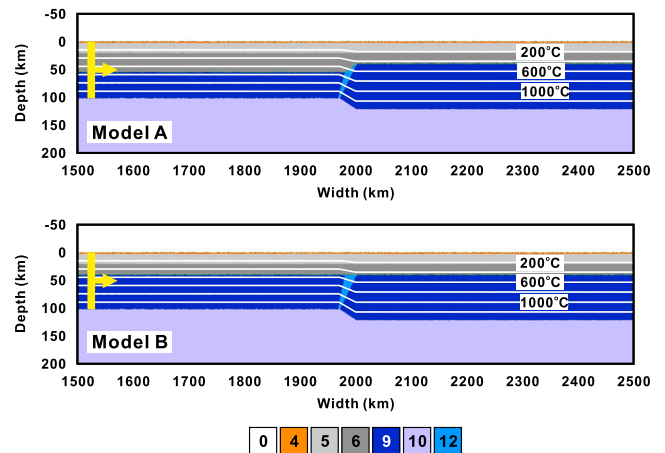


Figure 2. Two typical model setups. Models A and B correspond to the model setups with a 15 km crustal difference and without crustal thickness difference, respectively. The color code represents the different rock types, with 0, sticky air; 4, sediment; 5, upper continental crust; 6, lower continental crust; 9, lithospheric mantle; 10, asthenosphere; and 12, weak zone mantle. The yellow arrow denotes the direction of convergence force. White lines are isotherms measured in Celsius.

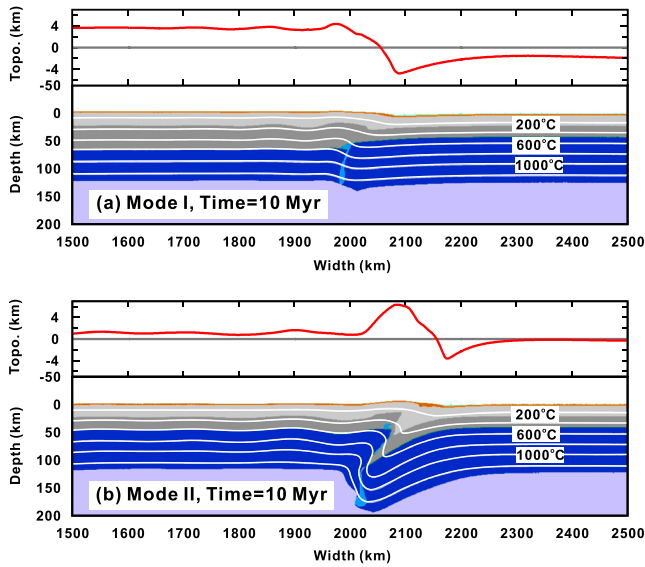


Figure 3. Composition evolution and corresponding topographies for Models A and B after 10 Ma of convergence. Isotherms are shown as white lines for every 200°C. (a) The steep margin regime; (b) the continental underthrust regime.

the two blocks, is characterized by continental lithosphere underthrusting (Figure 3b). The phenomenon is similar to the numerical models of continental subduction [e.g., *Li et al.*, 2010]. In this mode, underthrusting of the cratonic basin is accompanied by rightward movement of the upper crust of the plateau. This mode demonstrates coherent buckling of the crust and lithospheric mantle of the plateau. Rightward convergence together with lateral density contrast between the lithospheric blocks results in the cratonic lithosphere bending, retreating, and initiating underthrusting. The lithospheric architecture in this case resembles that of the Tian Shan, in which the cratonic Tarim Basin lithosphere may have been subducted beneath the Tian Shan [*Lei and Zhao*, 2007; *Omuralieva et al.*, 2009]. In this case, although steep topography is developed at the cratonic margin, the topographic profile is characterized by uplift only above the junction of the two blocks, and a distributed high-elevation plateau is not formed, which is also consistent with the Tian Shan.

[12] The difference in lithospheric architecture and topography between Mode-I and Mode-II (Table 2) clearly indicates that the preconvergence crustal thickness contrast between lithospheric blocks is a primary driver for the growth of steep topographic margin in intraplate settings.

[13] The lithospheric thermal state also plays an important role in controlling intracontinental convergence processes [e.g., *Beaumont et al.*, 2001; *Toussaint et al.*, 2004]. To identify the influence of thermal contrast of lithospheres on the formation of steep margins, we conducted one more experiment (Figure 4). In this model, there is no difference for both crustal thickness and lithosphere thermal state between the two blocks. Because the initial geotherms of the two blocks are the same, there is thus no difference in the lithospheric strength at the beginning. In this case, the lithospheric architecture is controlled by the location and geometry of the lithospheric weak zone, which causes the lithosphere of the “plateau block” to be

thrust over the cratonic basin lithosphere. The overriding block remains almost intact, while the lower part of the cratonic lithosphere is underthrust, while the upper part is overthrust onto the plateau block. The topographies are similar to those in Mode II, just significantly elevating the contacting zone. This model shows that, with uniform crustal thickness, the thermal contrast between two convergent lithospheric blocks has the effect of controlling the rate of underthrust but does not generate a plateau or steep topography at the margin.

[14] Our numerical experiments demonstrate that the crustal thickness contrast between the plateau and the cratonic basin is the primary factor in producing a steep topography margin. The lithospheric thermal contrast is subordinate to the crustal thickness and has a dominant influence only on the rate of overthrusting, as with hotter lithosphere more strain is taken up by lithospheric thickening and less by overthrusting. By comparing Figures 3b and 4d, we can see that a higher temperature gradient dramatically reduces the strength of the “plateau lithosphere” on the whole and makes it more deformable (e.g., Figure 3b), while a lower temperature gradient makes the “plateau lithosphere” behave more like a rigid plate (e.g., Figure 4d). An increase of the lower-crustal thickness also reduces the lithospheric strength but on a local scale, because the plagioclase-dominated lower crust in our model is more

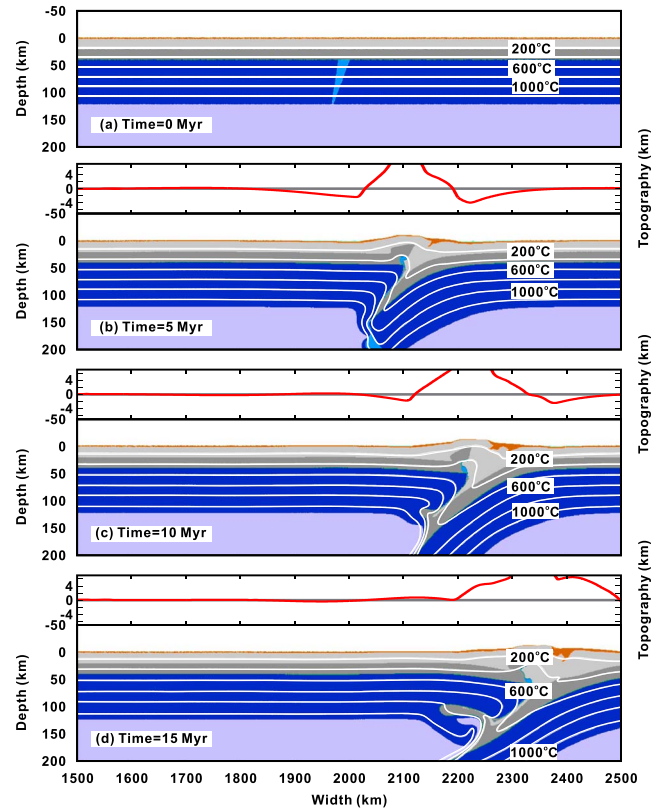


Figure 4. Temporal evolution of Model C showing composition and temperature fields at (a) 0 Myr, (b) 5 Myr, (c) 10 Myr and (d) 15 Myr. Each snapshot is accompanied by topographic profile at top; isotherms are shown as white lines for each 200°C; time is shown starting from beginning of experiment.

deformable than olivine-dominated lithospheric mantle at the same temperature.

4. Discussion and Conclusions

[15] A hot continental lithosphere is mechanically weak [Burchfiel *et al.*, 2008], thin, and of low viscosity, while a thick crust further contributes to lithospheric weakness. Firstly, crustal heat production is a significant heat source in our model; thus, a thicker crust will generate warmer lithosphere. Secondly, the plagioclase-dominated lower crust in our model will flow more easily than olivine at the same temperature, further contributing to a weaker lithosphere. The relative thinness of the lithosphere and thickness of the crust also provide strong buoyancy forces. Therefore, in the case where a hot lithosphere with a thick crust juxtaposed against a thick lithosphere with thin crust (Figure 3a), a characteristic margin style forms, characterized by steep topography, as is observed in the eastern Tibetan margin. This comes about through two complementary processes: (1) thick crust and thin lithosphere each contribute to the positive buoyancy of the plateau region and generate a broad topographic uplift; and (2) relative weakness of the plateau region concentrates deformation (and thickening) on that side of the margin, while the cratonic basin remains largely undeformed. The deformation style is predominated by pure shear; thus, a uniformly elevated topography can be produced (Figure 3a).

[16] Our modeling suggests that crustal thickness variation is the overriding factor in determining the existence of steep topography and plateau development. In the absence of preceding crustal thickness variations, plateaus are not formed, and the gravity instability caused by a thermally induced density contrast leads to cratonic lithosphere sinking and underthrusting along the weak zone (Figure 3b). The topography in this case uplifts significantly only above the underthrusting zone, and a high-elevation plateau is not formed (Figure 3b). A potential example of this style of intraplate cratonic margin may be the margin of the Tarim Basin with the Tian Shan, where topographic growth is focused in a narrow region close to the margin, the cratonic lithosphere may be subducting, and crustal thickness is not markedly different between the two blocks [Lei and Zhao, 2007; Omuralieva *et al.*, 2009].

[17] Lithospheric temperature (and thickness) variations are less important, presumably due to the reduced buoyancy forces, although they are still influential in controlling the rate of overthrusting. Geological and geophysical observations indicate that there are several major common points between the eastern Tibetan margin adjacent to the Sichuan Basin and the northern Tibetan margin adjacent to the Tarim Basin, such as an abrupt Moho offset underneath the range front [Zhang *et al.* [2009]; Xiao *et al.* [2002]; see Figures 1a, 1c, and 1e), steep topographic gradient [Clark and Royden, 2000], little convergence perpendicular to margins [Gan *et al.* 2007], and the existence of major strike slip faults and high-strength lithosphere (rigid craton) at the basin side. Thus, these two intracontinental convergent margins can be classified as steep topography type cratonic-plateau margins (eastern Tibetan-type margin), although they have different climates and erosion histories [Hetzel, 2013].

[18] The topography along the northeastern Tibetan margin decreases from ~4.5 km to ~500 m over a distance more than 1500 km (Figure 1b). In contrast to the eastern

Tibetan-type margin, it is obviously a smooth margin. This feature is probably caused by a lack of significant Moho offset beneath the range front (Figure 1b).

[19] Our numerical experiments demonstrate that the eastern Tibetan-type steep margins are an inherent product when a hot/weak lithosphere with thick crust converges with a cold/strong lithosphere with relatively thin crust. Furthermore, it is apparent that the crustal thickness prior to convergence is the primary factor in determining whether the lithosphere responds by building an elevated plateau or whether continental underthrust is initiated. Although it has been potentially able to contribute to the crustal thickness contrast between the two colliding plates, the lower-crustal flow is not a prerequisite for the growth of a steep topography margin.

[20] **Acknowledgments.** This research was supported by the National Natural Science Foundation of China (Nos. 41004039 and 41021063), the Ministry of Science and Technology of China (No. 2011CB808904), and the Ministry of Land and Resources of China (SinoProbe-02-02 or 201011041, SinoProbe-03-02 or 201011047). We are very grateful to Manuele Faccenda and an anonymous reviewer for their constructive comments. We thank Liu Lijun and Xu Tao for their helpful suggestions. We also thank Gan Weijun for providing the GPS data and Wang Peng for his help on redrawing Figures 2 to 4. Figure 1 was generated with GMT package developed by Paul Wessel and Walter H. F. Smith. All the simulations were run on the ETH Brutus cluster.

[21] The Editor thanks Manuele Faccenda and an anonymous reviewer for their assistance in evaluating this paper.

References

- Avouac, J. P., and E. B. Burov (1996), Erosion as a driving mechanism of intracontinental mountain growth, *JGR-Solid Earth*, *101*, 17,747–17,769.
- Beaumont, C., R. A. Jamieson, M. H. Nguyen, and B. Lee (2001), Himalayan tectonics explained by extrusion of a low-viscosity crustal channel coupled to focused surface denudation, *Nature*, *414*, 738–742.
- Burchfiel, B. C., Z. Chen, Y. Liu, and L. Royden (1995), Tectonics of the Longmen Shan and adjacent regions, Central China, *Int. Geol. Rev.*, *37*(8), 661–735.
- Burchfiel, B. C., L. H. Royden, R. D. van der Hilst, B. H. Hager, Z. Chen, R. W. King, C. Li, J. Lu, H. Yao, and E. Kirby (2008), A geological and geophysical context for the Wenchuan earthquake of 12 May 2008, Sichuan, People's Republic of China, *GSA Today*, *18*, doi:10.1130/GSATG18A.1.
- Burg, J. P., and T. V. Gerya (2005), The role of viscous heating in Barrovian metamorphism of collisional orogens: Thermomechanical models and application to the Lepontine Dome in the Central Alps, *J. Metamorph. Geol.*, *23*, 75–95.
- Clark, M. K., and L. H. Royden (2000), Topographic ooze: Building the eastern margin of Tibet by lower crustal flow, *Geology*, *28*(8), 703–706.
- Fielding, E. J., and D. McKenzie (2012), Lithospheric flexure in the Sichuan Basin and Longmen Shan at the eastern edge of Tibet, *Geophys. Res. Lett.*, *39*, L09311, doi:10.1029/2012GL051680.
- Fielding, E., B. Isacks, M. Barazangi, and C. Duncan (1994), How flat is Tibet?, *Geology*, *22*, 163–167.
- Gan, W., P. Zhang, Z. Shen, Z. Niu, M. Wang, Y. Wan, D. Zhou, and J. Cheng (2007), Present-day crustal motion within the Tibetan Plateau inferred from GPS measurements, *J. Geophys. Res.*, *112*, B08416, doi:10.1029/2005JB004120.
- Gerya, T. V., and D. A. Yuen (2003), Characteristics-based marker-in-cell method with conservative finite-differences schemes for modeling geological flows with strongly variable transport properties, *Phys Earth Planet In.*, *140*, 295–320.
- Hetzel, R. (2013), Active faulting, mountain growth, and erosion at the margins of the Tibetan Plateau constrained by in situ-produced cosmogenic nuclides, *Tectonophysics*, *582*, 1–24.
- Holbig, E. S., and T. L. Grove (2008), Mantle melting beneath the Tibetan Plateau: Experimental constraints on ultrapotassic magmatism, *J. Geophys. Res.*, *113*, B04210, doi:10.1029/2007JB005149.
- Hu, J., H. Yang, L. Wen, and G. Li (2011), S receiver function analysis of the crustal and lithospheric structures beneath eastern Tibet, *Earth Planet. Sci. Lett.*, *306*, 77–85.

- Hubbard, J., and J. H. Shaw (2009), Uplift of the Longmen Shan and Tibetan plateau, and the 2008 Wenchuan ($M=7.9$) earthquake, *Nature*, 458, 194–197, doi:10.1038/nature07837.
- Lei, J., and D. Zhao (2007), Teleseismic P -wave tomography and the upper mantle structure of the central Tien Shan orogenic belt, *Phys Earth Planet In*, 162, 165–185.
- Li, C., R. D. van der Hilst, and M. N. Toksoz (2006), Constraining spatial variations in P -wave velocity in the upper mantle beneath SE Asia, *Phys Earth Planet In*, 154, 180–195.
- Li, Z. H., T. V. Gerya, and J. P. Burg (2010), Influence of tectonic overpressure on P - T paths of HP-UHP rocks in continental collision zones: Thermomechanical modeling, *J. Metamorph. Geol.*, 28, 227–247.
- Liu, M., W. D. Mooney, S. Li, N. Okaya, and S. Detweiler (2006), Crustal structure of the northeastern margin of the Tibetan plateau from the Songpan-Ganzi terrane to the Ordos basin, *Tectonophysics*, 420, 253–266.
- Meng, Q. R., J. M. Hu, E. Wang, and H. J. Qu (2006), Late Cenozoic denudation by large-magnitude landslides in eastern edge of Tibetan Plateau, *Earth Planet. Sci. Lett.*, 243, 252–267.
- Omuralieva, A., J. Nakajima, and A. Hasegawa (2009), Three-dimensional seismic velocity structure of the crust beneath the central Tien Shan, Kyrgyzstan: Implications for large- and small-scale mountain building, *Tectonophysics*, 465, 30–44, doi:10.1016/j.tecto.2008.10.010.
- Ranalli, G. (1995), *Rheology of the Earth*, Chapman & Hall Press, London, U. K., pp. 413.
- Robert, A., J. Zhu, J. Vergne, R. Cattin, L. S. Chan, G. Wittlinger, G. Herquel, J. de Sigoyer, M. Pubellier, and L. D. Zhu (2010), Crustal structures in the area of the 2008 Sichuan earthquake from seismologic and gravimetric data, *Tectonophysics*, 491, 205–210.
- Royden, L. H., B. C. Burchiel, R. W. King, E. Wang, Z. Chen, F. Shen, and Y. Liu (1997), Surface deformation and lower crustal flow in eastern Tibet, *Science*, 276, 788–790.
- Toussaint, G., E. Burov, and J. P. Avouac (2004), Tectonic evolution of a continental collision zone: A thermomechanical numerical model, *Tectonics*, 23, TC6003, doi:10.1029/2003TC001604.
- Wallis, S., T. Tsujimori, M. Aoya, T. Kawakami, K. Terada, K. Suzuki, and H. Hyodo (2003), Cenozoic and Mesozoic metamorphism in the Longmenshan orogen: Implications for geodynamic models of eastern Tibet, *Geology*, 31, 745–748.
- Wang, C. Y., W. B. Han, J. P. Wu, H. Lou, and W. W. Chan (2007), Crustal structure beneath the eastern margin of the Tibetan Plateau and its tectonic implications, *J. Geophys. Res.*, 112, B07307, doi:10.1029/2005JB003873.
- Wang, E., E. Kirby, K. P. Furlong, M. van Soest, G. Xu, X. Shi, P. J. J. Kamp, and K. V. Hodges (2012), Two-phase growth of high topography in eastern Tibet during the Cenozoic, *Nat. Geosci.*, 5, 640–645, doi:10.1038/NGEO1538.
- Xiao, X., X. Liu, R. Gao, and Z. Luo (2002), Lithospheric structure and tectonic evolution of the West Kunlun and its adjacent areas—Brief report on the South Tarim-West Kunlun multidisciplinary geosciences transect, *Geological Bulletin of China*, 21(2), 63–68.
- Yin, A., and T. M. Harrison (2000), Geological evolution of the Himalayan Tibetan orogen, *Annu. Rev. Earth Planet. Sci.*, 28, 211–280.
- Zhang, Z., Y. Wang, Y. Chen, G. A. Houseman, X. Tian, E. Wang, and J. Teng (2009), Crustal structure across Longmenshan fault belt from passive source seismic profiling, *Geophys. Res. Lett.*, 36, L17310, doi:10.1029/2009GL039580.
- Zhang, Z., X. Yuan, Y. Chen, X. Tian, R. Kind, X. Li, and J. Teng (2010), Seismic signature of the collision between the East Tibetan escape flow and the Sichuan basin, *Earth Planet. Sci. Lett.*, 292, 254–264.
- Zhao, J., et al. (2010), The boundary between the Indian and Asian tectonic plates below Tibet, PNAS, doi/10.1073/pnas.1001921107.
- Zhao, W., et al. (2011), Tibetan plate overriding the Asian plate in central and northern Tibet, *Nat. Geosci.*, 4, doi:10.1038/NGEO1309.